## Title

Light-promoted aromatic denitrative chlorination



## Authors

Liang, Tiantian
Lyu, Zhen
Wang, Ye
et al.

## Publication Date

2025-01-20

## DOI

10.1038/s41557-024-01728-1

nature chemistry

Article

https://doi.org/10.1038/s41557-024-01728-1

# Light-promoted aromatic denitrative chlorination

Received: 23 May 2024

Accepted: 19 December 2024

Published online: 20 January 2025

Check for updates

Tiantian Liang[1,5], Zhen Lyu[2,5], Ye Wang[1], Wenyan Zhao[1], Ruocheng Sang[3], Gui-Juan Cheng[2] ✉ & Fei Ye[1,4] ✉

Nitroarenes are readily accessible bulk chemicals and can serve as versatile starting materials for a series of synthetic reactions. However, due to the inertness of the $C_{Ar}$–$NO_2$ bond, the direct denitrative substitution reaction with unactivated nitroarenes remains challenging. Chemists rely on sequential reduction and diazotization followed by the Sandmeyer reaction or the nucleophilic aromatic substitution of activated nitroarenes to realize nitro group transformations. Here we develop a general denitrative chlorination reaction under visible-light irradiation, in which the chlorine radical replaces the nitro moiety through the cleavage of the $C_{Ar}$–$NO_2$ bond. This practical method works with a wide range of unactivated nitro(hetero) arenes and nitroalkenes, is not sensitive to air or moisture and can proceed smoothly on a decagram scale. This transformation differs fundamentally from previous nucleophilic aromatic substitution reactions under thermal conditions in both synthesis and mechanism. Density functional theory calculations reveal the possible pathway for the substitution reaction.

Nitro(hetero)arenes are one of the most abundant chemical feedstocks in organic synthesis[1,2], playing a vital role in both academic research[3] and industrial production[4]. Their widespread availability stems from their efficient preparation through electrophilic aromatic substitution, a reaction known for its broad substrate scope and scalability, making it suitable for diverse chemical environments and applications[5]. Due to these characteristics, nitroarenes are invaluable intermediates in the production of pharmaceuticals, agrochemicals and functional materials. The nitro moiety can be smoothly transferred into various aniline derivatives or *N*-containing cyclic compounds, which are essential motifs in drug discovery and material science, through well-established thermal conditions[6–12]. However, the light-induced transformation of nitrobenzene derivatives has gained significant attention in the past decade[13]. Advances in this field have widely expanded the utility of nitroarenes, leveraging the nitro moiety as a versatile functional handle in photochemical processes. These transformations have broadened the scope of applications, allowing the nitro group to function as a hydrogen atom transfer (HAT) reagent[14], as an oxygen atom transfer reagent[15–17] and even as a nitrene precursor[18–21], enabling distinct reactivity patterns that are otherwise inaccessible in thermal reactions (Fig. 1a). Such transformations highlight the growing importance of nitroarenes in green and sustainable chemistry, as many of these transformations are carried out under mild, eco-friendly conditions, reducing the need for harsh reagents and forcing temperatures. However, the nitro moiety was rarely suitable as a general leaving group in direct substitution reactions due to the conjugation effect. This limitation arises primarily from the conjugative stabilization of the nitro group within the aromatic system, making it much less reactive compared to other electron-withdrawing groups, such as halides. Alternatively, chemists often use the multistep sequence of reduction, diazotization and Sandmeyer reaction to indirectly realize functional group interconversion[22–24]. While effective, these three-step protocols often suffer from poor atom economy and the generation of an excess amount of waste as well as an explosive diazonium salt intermediate (Fig. 1b). Thus, the direct conversion from Ar–$NO_2$ to Ar–FGs (FG, functional group) was a long-standing challenge that remained unexplored.

[1]CCNU-uOttawa Joint Research Centre, Key Laboratory of Pesticide & Chemical Biology, Ministry of Education, College of Chemistry, Central China Normal University, Wuhan, China. [2]Warshel Institute for Computational Biology, School of Medicine, The Chinese University of Hong Kong, Shenzhen, China. [3]Institute for Neurodegenerative Diseases, University of California, San Francisco, CA, USA. [4]Wuhan Institute of Photochemsitry and Technology, Wuhan, China. [5]These authors contributed equally: Tiantian Liang, Zhen Lyu. ✉e-mail: chengguijuan@cuhk.edu.cn; yef@ccnu.edu.cn

https://doi.org/10.1038/s41557-024-01728-1

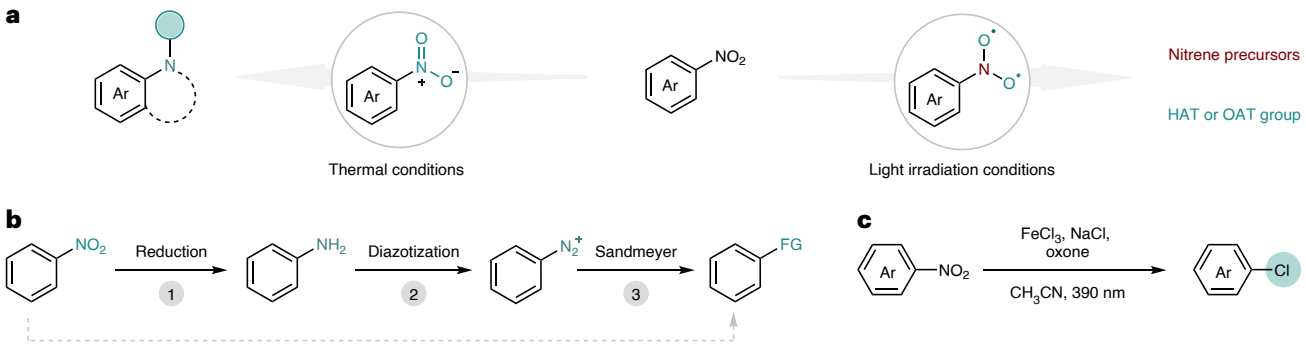


**Fig. 1 | Strategies for the transformation of nitroarenes. a**, Light-induced transformation of nitrobenzene. Nitro group can be employed as a HAT reagent, oxygen atom transfer (OAT) reagent or nitrene precursors. **b**, Classical three-step denitrative transformation (reduction–diazotization–Sandmeyer reaction). **c**, Light-promoted aromatic denitrative substitution (this work). Aromatic denitrative chlorination reaction occurs in one step with unactivated nitroarenes in the decagram scale under air, without the consumption of noble metals or photoredox catalysts.

Traditionally, nucleophilic aromatic substitution ($S_NAr$) reactions directly transfer the nitro moiety to other functional groups. However, the relatively high activation barrier associated with these substitution reactions limits the substrate scope to electron-deficient nitroarenes (that is, activated nitroarenes) and necessitates the use of forcing conditions, such as a high temperature as well as strong basic media[25]. Since 2017, the Nakao group further expanded the bonding manner starting from nitroarenes through $C_{Ar}$–$NO_2$ bond cleavage. They developed a cross-coupling strategy by using a Pd/BrettPhos catalytic system to realize C–C and C–N bond formation by treating the nitro group as a pseudo halide[26–28]. These methods constituted a notable advancement, yet opportunities for further optimization still remain, particularly concerning the need for precious metal catalysts. Despite these findings, the conversion of nitro groups to other high-value functionalities, particularly those with diverse reactivity such as halides, without the consumption of expensive catalysts still poses a challenge for common nitroarenes (only 1-nitronaphtalene can be transferred to 1-chloronaphtalene under light irradiation[29], and only 4-nitrobiphenyls can be transferred to 4-cyanobiphenyls under 254 nm irradiation[30]). In this context, we developed a visible-light-induced denitrative chlorination reaction that efficiently converts unactivated nitroarenes and nitroalkenes into chlorinated products without the need for photoredox catalysts or noble metal catalysts[31–34]. This method cleaves the $C_{Ar}$–$NO_2$ bond under mild conditions, to form $C_{Ar}$–Cl bonds directly (Fig. 1c). Unlike traditional $S_NAr$ reactions, which require high temperature and electron-deficient substrates, this photochemical approach proceeds under ambient conditions, expanding the scope to include a broader range of (hetero) arenes and alkene systems. This innovation opens up practical avenues for the efficient transformation of nitroarenes and nitroalkenes into high-value halogenated products, which are key intermediates in pharmaceutical and materials chemistry.

## Results and discussion

### Conditions and scope of denitrative chlorination

The denitrative chlorination reaction of 4-nitrobiphenyl using the first-row transition metal chlorides as the catalysts in acetonitrile (MeCN) was thoroughly investigated under irradiation with violet light-emitting diodes (LEDs; 390 nm). The reaction leverages the photoinduced ligand-to-metal charge transfer (LMCT) of the first-row transition metal chlorides to generate reactive free chlorine radicals[35], which are crucial to facilitating the denitrative chlorination process (Supplementary Table 1). We identified ferric chloride ($FeCl_3$) as a promising catalyst candidate that could provide the target denitrative chlorination product in an impressive 89% isolated yield (Supplementary Table 1, entry 1). But, if the reaction was conducted at room temperature, the yield dramatically dropped to 22%, demonstrating that elevated temperature is key for achieving both full conversion of the starting material and high yields of the desired product (Supplementary Table 1, entry 2). The control experiments revealed that without the presence of both $FeCl_3$ and the oxidant oxone, only trace amounts of the chlorination product were formed, highlighting the necessity of these components for efficient reaction progression (Supplementary Table 1, entry 3). Furthermore, the addition of sodium chloride, combined with oxone, significantly boosted the reaction yield, suggesting that the increased concentration of chlorine radicals was responsible for the improved efficiency (Supplementary Table 1, entries 4 and 5). The denitrative chlorination reaction can still proceed with only sodium chloride and oxone, indicating that ferric chloride is not necessary for the transformation but could increase the efficiency of the reaction (Supplementary Table 1, entry 6). We also proved that the light irradiation was a critical factor in this transformation, not only for promoting the reaction but also for ensuring the site selectivity of the chlorination (Supplementary Table 1, entry 7). While we observed that the oxidative generation of chlorine radicals could still proceed without light, the yield of nitro to chloro substitution was notably lower, and C–H chlorination products also formed in these conditions, underscoring the essential role of light in steering the reaction towards the desired product (Supplementary Table 1, entry 8). Interestingly, the reaction could be carried out under ambient air atmosphere, to give a very similar yield (Supplementary Table 1, entry 9), demonstrating the robustness and practicality of our protocol for denitrative chlorination.

With the optimized conditions in hand, the substrate scope and functional group tolerance of this transformation were then investigated (Table 1). Electron-withdrawing groups such as cyano (**1**), halogens (**2** and **9**), carbonyls (**10**) and trifluoromethyls (**6** and **8**) can be tolerated under standard conditions, delivering the chlorinated products in moderate to good yields. Moreover, electron-donating groups such as free hydroxyls (**3**) or protected hydroxyls (**15**, **23** and **24**), phenyls (**4**–**7** and **22**) and ether (**16**) were also compatible and provided the products at up to 89% yield. Most of those substrates failed to give the desired products under thermally induced $S_NAr$ reaction conditions. Free amines would not survive under the current conditions, although protected amines such as phthalimide (**11**) and amide derivatives (**20**, **21** and **25**) are compatible with the transformation. Additionally, heterocycle substituents, such as thiophene (**17**), oxazole (**18**) and pyrazole (**19**), were effectively converted to their chlorinated analogues in decent yields. The clofibrate derivative (**26**) was also very compatible. Denitrative chlorination can also proceed for condensed rings such as naphthalene derivatives (**27** and **28**), fluorene (**29**), fluorenone (**30**), phenanthrene (**31**) and dibenzofuran (**32**).

https://doi.org/10.1038/s41557-024-01728-1

**Table 1 | Substrate scope of denitrative chlorination**

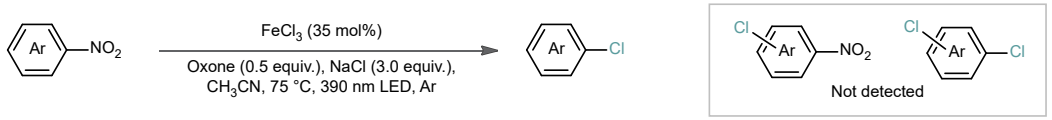


Aryl rings

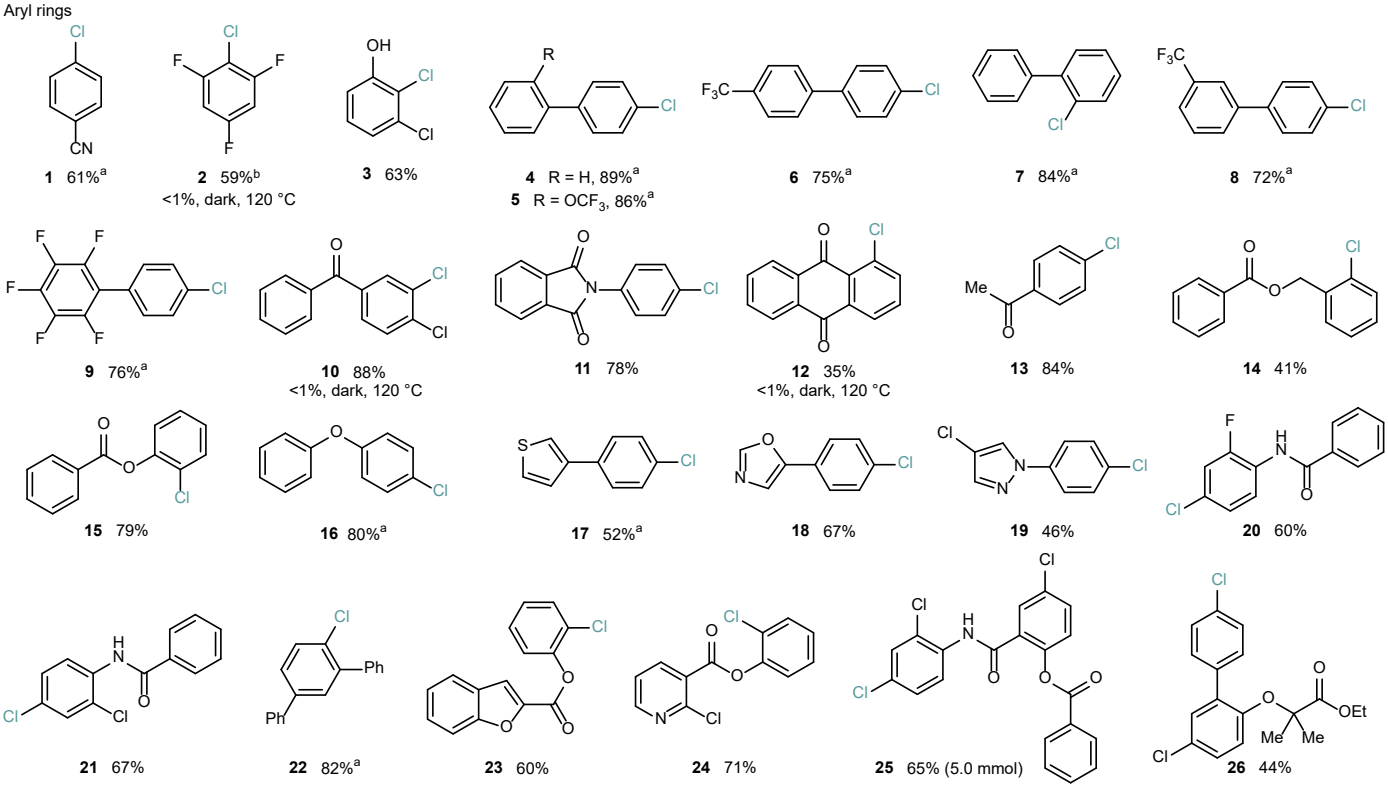


Condensed rings and heterocycles

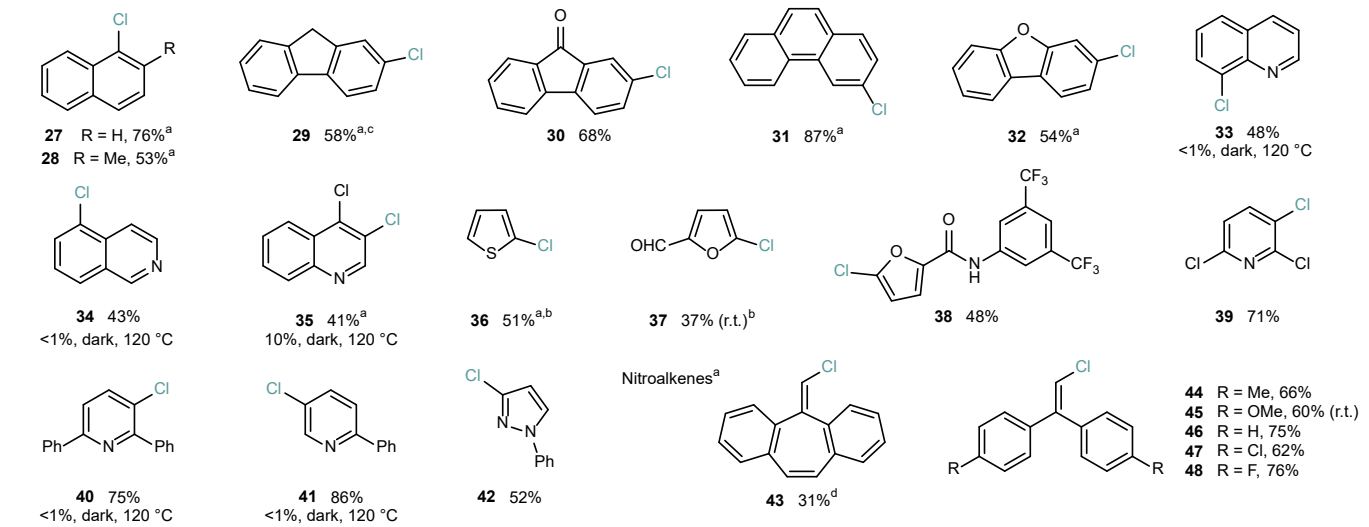


Unless noted otherwise, the reactions were conducted in 0.2 mmol nitroarene, $FeCl_3$ (35 mol%), oxone (50 mol%), NaCl (3.0 equiv.) and $CH_3CN$ (0.1 M) under 390 nm LED irradiation at 75 °C for 48 h. r.t., room temperature. [a]0.2 mmol nitroarene, $FeCl_3$ (1.0 equiv.) in 0.1 M $CH_3CN$. [b]GC yields using a calibration curve. [c]Product contains unseparable chlorination product (**29**/C–H chlorination product = 5:1). [d]5-(nitromethylene)-10,11-dihydro-5*H*-dibenzo[a,d][7]annulene was used as starting material.

The transformation of heterocycles such as quinolines (**33**), isoquinolines (**34** and **35**), thiophenes (**36**), furans (**37** and **38**), pyridines (**39**–**41**) and pyrazoles (**42**) was also performed successfully. Similarly, nitroalkenes (**43**–**48**) were successfully employed as substrates with different electron-effect substituents and converted to chlorinated alkenes in moderate yields. To verify the difference between the light-induced denitrative chlorination with traditional aromatic nucleophilic substitution, we carried out the chlorination reaction at 120 °C without light irradiation. For nitroarenes bearing one more electron-withdrawing group (**2**, **10**, **12**, **33**–**35**, **40** and **41**), which are prone to undergo a thermally induced $S_NAr$ reaction, most of them failed to give denitrative chlorination products.

https://doi.org/10.1038/s41557-024-01728-1

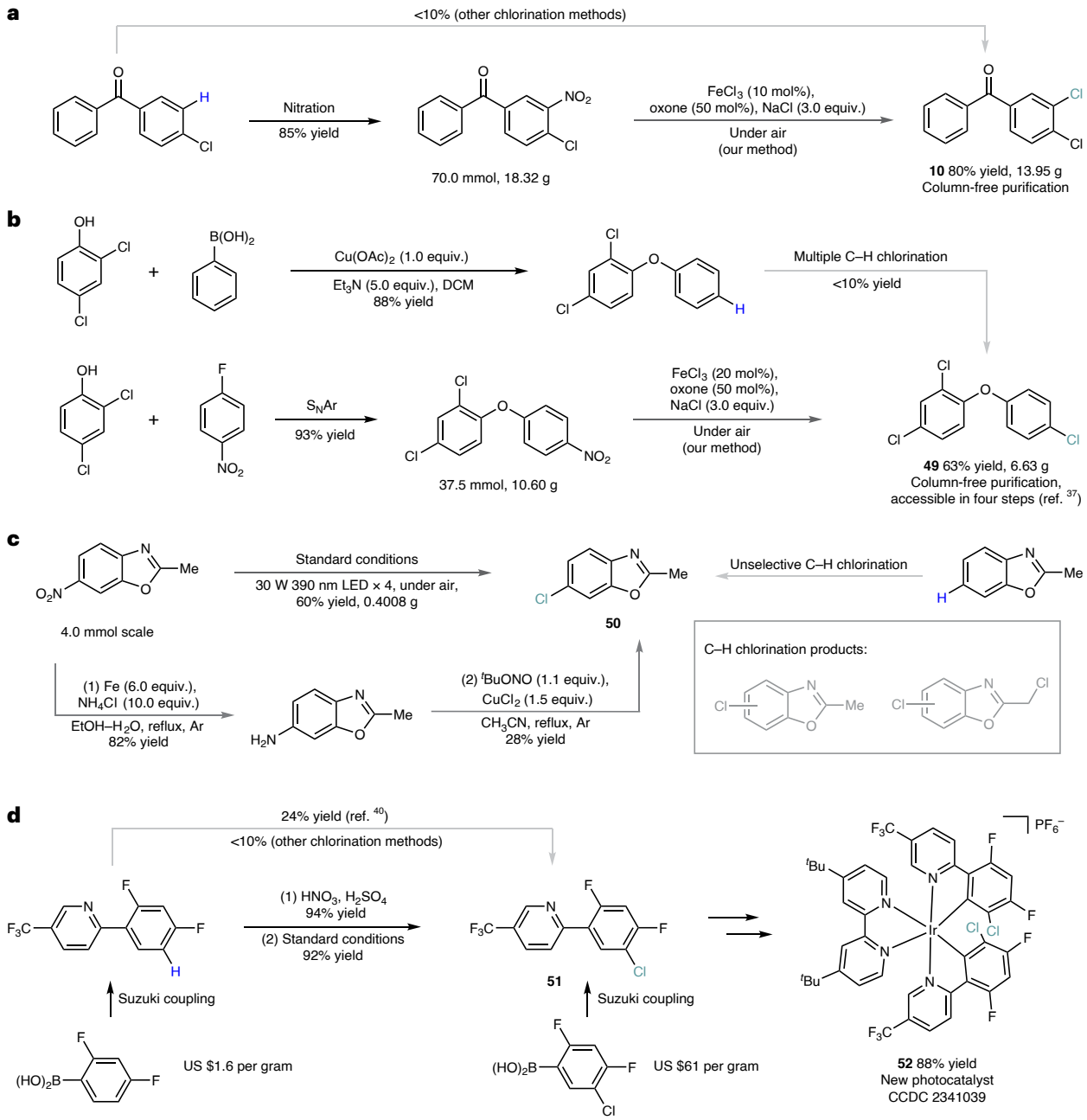


**Fig. 2 | Examples of synthetic applications. a**, Scaled up denitrative chlorination of electron-deficient arene and comparison with direct C–H chlorination. **b**, Scaled up denitrative chlorination of electron-rich arene and comparison with direct C–H chlorination. DCM, dichloromethane. **c**, Comparison of denitrative chlorination of heterocyclic arene with its three-step synthesis as well as direct C–H chlorination. The Sandmeyer reaction had low efficiency, and C–H chlorination was unselective. **d**, Synthesis of Ir[dF(Cl)(CF$_3$)ppy]$_2$(dtbbpy)PF$_6$. A sequence of Suzuki coupling, nitration and denitrative chlorination was used to prepare the ligand. CCDC, Cambridge Crystallographic Data Centre.

## Synthetic applications of denitrative chlorination

To further demonstrate the synthetic value of this strategy, the capacity for our protocol to markedly simplify the synthesis of aryl chlorides was shown through three case studies. The first is 3,4-dichlorobenzophenone **10**. Starting from commercially available 4-chlorobenzophenone, the target molecule **10** can be synthesized through Jiao's method, albeit in less than 10% isolated yield[36]. However, the nitration reaction of 4-chlorobenzophenone is selective and high yielding. We could then prepare compound **10** by using our denitrative chlorination method at a 14 g scale (80% yield) under air atmosphere, with a concise, column-chromatography-free workup procedure, which required only filtration, extraction and decolorization to afford the denitrative chlorination product (Fig. 2a). In the second case study, the triclosan precursor **49** was also chosen as a target compound. With our method, the starting material nitrobiphenyl ether can be prepared by S$_N$Ar reaction in more than 90% yield, and the following denitrative chlorination reaction provides simplicity in operation and workup, on a multigram scale with 63% yield under air atmosphere. Alternatively, compound **49** can be made through a four-step sequence of S$_N$Ar reaction, reduction, diazotization and Sandmeyer reaction[37], or through an unselective aromatic C–H chlorination reaction with relatively low efficiency[38], and the starting material must be made through a coupling reaction with a stoichiometric amount of copper salt (Fig. 2b). In the third case study, a heterocyclic compound 2-methylbenzoxazole

https://doi.org/10.1038/s41557-024-01728-1

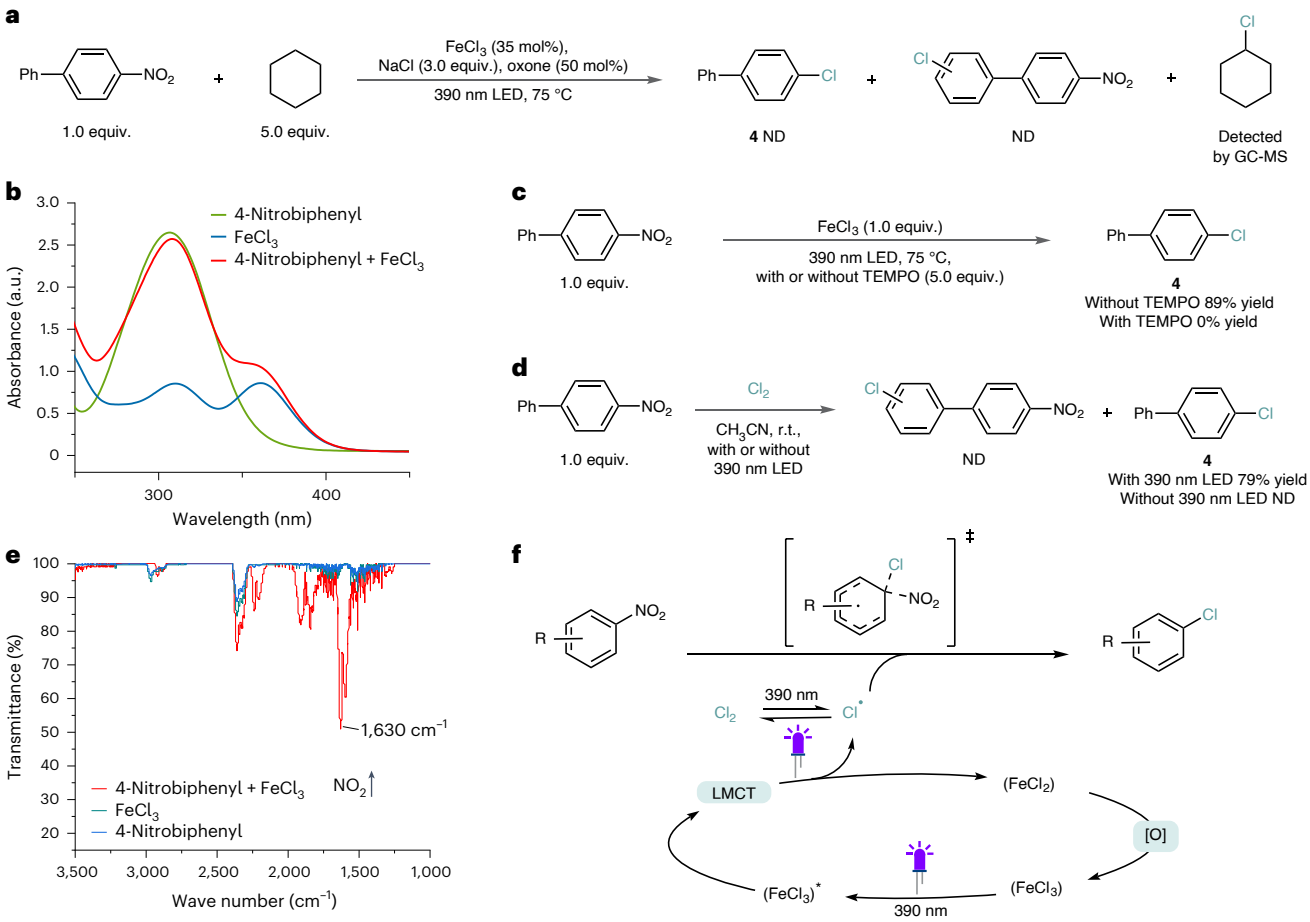


**Fig. 3 | Mechanistic investigations. a**, Competition study with cyclohexane. Chlorocyclohexane was detected and no denitrative chlorination product was observed. ND, not detected. **b**, UV–visible absorption spectrum. $FeCl_3$ was irradiated at around 390 nm. **c**, Radical quenching experiment. No desired product was observed when TEMPO was added to the reaction mixture. **d**, Reaction with $Cl_2$ with or without light. The denitrative chlorination product was observed under 390 nm LED irradiation. **e**, IR absorption spectrum. An online IR spectrometer with a triglycine sulfate detector and a custom-built gas cell was used. **f**, Plausible mechanism. The in situ generated chlorine radicals by LMCT undergo radical substitution reactions to generate the corresponding aryl chloride products and $NO_2$ gas.

was shown. Direct C–H chlorination failed to yield the desired product **50**, due to the formation of regioisomers and the chloromethyl product[36,38–40] (Fig. 2c). As the nitro moiety can be introduced *para* to the nitrogen atom with high regioselectivity, we could then use the denitrative chlorination method to access compound **50** in 63% isolated yield. We also conducted a comparison reaction with a classical three-step method, and the result showed that only 28% yield was obtained when **50** was synthesized by the Sandmeyer reaction. Finally, we successfully modified the photocatalyst $Ir[dF(CF_3)ppy]_2(dtbbpy)PF_6$ by a selective nitration–denitrative chlorination protocol. Using a traditional cross-coupling method to obtain the chlorinated phenylpyridine ligand typically requires expensive chlorinated boronic acid (US $61 per gram). However, our method provided a low-cost alternative. After selective nitration of phenylpyridine in excellent yield, the denitrative chlorination reaction could be carried out successfully to deliver chlorinated phenylpyridine in 92% isolated yield. Subsequently, we synthesized photocatalyst $Ir[2\text{-}(2,4\text{-difluoro-}3\text{-chlorophenyl})\text{-}5\text{-}(trifluoromethyl)pyridine]_2(4,4'\text{-di-tert-butyl-}2,2'\text{-bipyridine})PF_6$ ($Ir[dF(Cl)(CF_3)ppy]_2(dtbbpy)PF_6$) in two steps with 88% yield. Moreover, the C–H chlorination of the initial phenylpyridine ligand also provided the product in only 24% yield[40] (Fig. 2d). Therefore, we believe that our denitrative chlorination reaction can provide a useful supplement to the C–H chlorination reaction and the Sandmeyer reactions.

## Mechanistic studies

To shed light on the mechanism of the denitrative chlorination reaction, a few experiments were conducted to study the reaction mechanism. The reaction of 4-nitrobiphenyl was examined in the presence of an excess amount of cyclohexane under standard conditions to capture chlorine radicals in the reaction mixture. Chlorocyclohexane was detected by gas chromatography/mass spectrometry (GC-MS) as expected, and the denitrative chlorination reaction was suppressed (Fig. 3a). These results imply that a chlorine radical is likely an intermediate in the reaction. What's more, the UV–visible absorption spectra of the reaction partners showed a notable absorbance corresponding to the excitation of $FeCl_3$ upon irradiation at 390 nm with LED, which is consistent with a literature report[35] (Fig. 3b). Moreover, no desired product was observed when the radical trapping reagent 2,2,6,6-tetramethyl-1-piperidinyloxy (TEMPO) was added to the reaction mixture, indicating that the reaction likely proceeded via a radical pathway (Fig. 3c). Furthermore, chlorine gas generated in situ from the mixture of hydrochloric acid and sodium hypochlorite was passed into the acetonitrile solution of 4-nitrobiphenyl. The denitrative chlorination product was also obtained with more than 80% isolated yield under purple-light irradiation. No products were observed without light irradiation, showing that the chlorine radical was most likely the key reaction intermediate (Fig. 3d). Additionally, in situ gaseous infrared (IR) analysis by an online IR spectrometer with a triglycine sulfate detector

https://doi.org/10.1038/s41557-024-01728-1

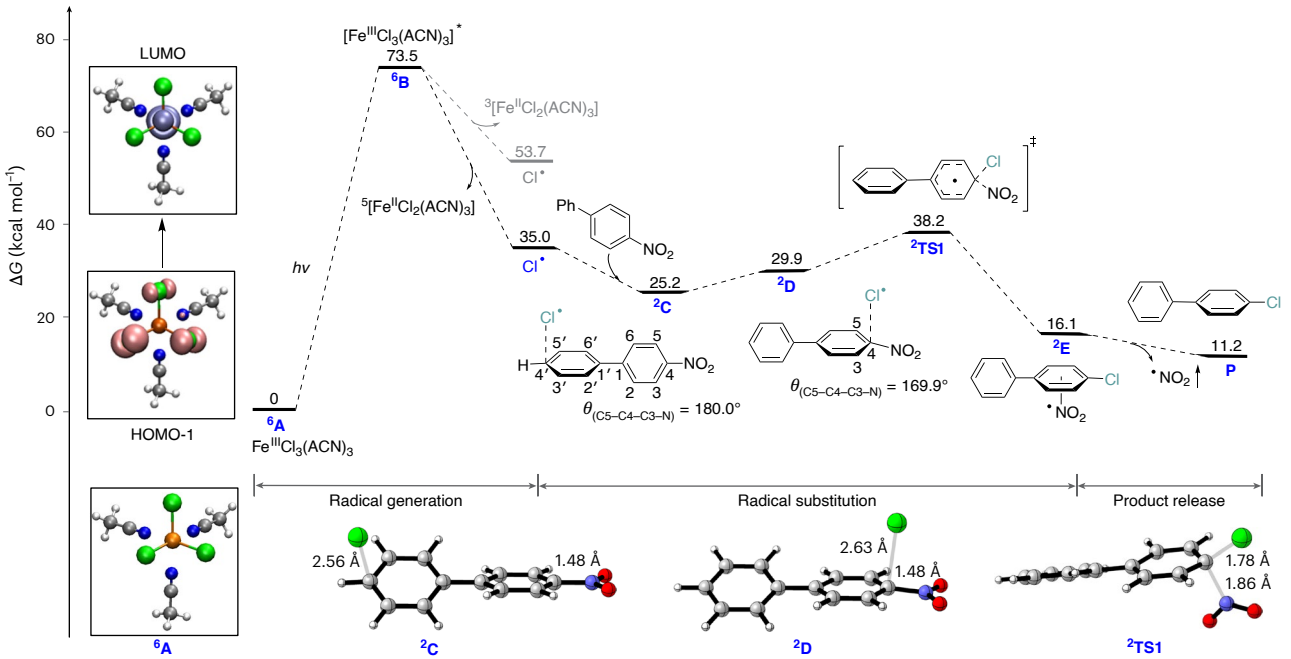


**Fig. 4 | Energy profile for the denitrative chlorination reaction.** Left: Orbitals shown are involved in the excitation process of $Fe^{III}Cl_3(ACN)_3$, indicating an electron transfer from the *p* orbital of Cl to the *d* orbital of iron. The spin state of each species is listed in the superscript at the top left corner of its label. LUMO, lowest unoccupied molecular orbital; HOMO, highest occupied molecular orbital; Δ*G*, relative Gibbs free energy; *h*, Planck's constant; *υ*, frequency of irradiated light. *θ*, dihedral angle defined by C3, C4, C5 and N.

and a custom-built gas cell showed an absorption peak at 1,630 $cm^{-1}$, which was consistent with the $NO_2$ signal reported in the literature[41]. This indicates the possibility for the generation of $NO_2$ gas from the reaction (Fig. 3e). Furthermore, the gas-phase electron paramagnetic resonance experiments of the reaction headspace further confirmed the formation of $NO_2$ gas from 4-nitrobiphenyl and iron chloride in acetonitrile solution under 390 nm irradiation (Supplementary Fig. 21). We also conducted light on/off experiments, the result of which showed the reaction ceases in the absence of light, which suggested that the reaction is less likely to proceed through a radical chain process (Supplementary Fig. 24). Based on these results, a plausible reaction mechanism was proposed as decsribed below (Fig. 3f). Denitrative chlorination with ferric chloride would begin with the dissociation of chlorine radicals via LMCT from the chloride ligand to the ferric ion under purple-light irradiation. The generated chlorine radicals then undergo a radical substitution reaction to generate the corresponding aryl chloride products and $NO_2$ gas. Alternatively, in the absence of iron, the chlorine radicals can also be formed by the excitation of chlorine gas from the direct oxidation of chloride anions.

### Density functional theory calculations

To gain a deeper understanding of the reaction mechanism, density functional theory (DFT) calculations were performed for the denitrative chlorination of substrate **4** (Fig. 4 and Supplementary Fig. 26). Upon the addition of iron chloride, various iron complexes form, including $[Fe^{III}Cl_4]^-$, $[Fe^{III}Cl_4(ACN)_2]^-$, $Fe^{III}Cl_3$ and $Fe^{III}Cl_3(ACN)_3$, where ACN is $CH_3CN$. Among these species, $Fe^{III}Cl_3(ACN)_3$ (species $^6$**A** in Fig. 4; the superscript shows the spin state of the species) is most likely to be excited upon irradiation, as its theoretical absorption wavelength (389 nm) closely matches the optical wavelength (390 nm) used in the experiment. Orbital analysis revealed that this absorption is attributed to LMCT[35,42,43], in which an electron transfers from the *p* orbital of Cl to the *d* orbital of iron (left panel, Fig. 4). Subsequent homolysis of the generated excited species $^6$**B** to afford the chlorine radical along with the quintet $^5[Fe^{II}Cl_2(CH_3CN)_3]$ is exergonic by 38.5 kcal $mol^{-1}$, which is more favourable by 18.7 kcal $mol^{-1}$ than homolysis with the triplet $^3[Fe^{II}Cl_2(CH_3CN)_3]$(refs. 44,45). The $^5[Fe^{II}Cl_2(CH_3CN)_3]$ can then be oxidized by oxone to regenerate $Fe^{III}Cl_3(ACN)_3$, while the Cl radical may attach to the C4′ of nitrobiphenyl to form a stable intermediate $^2$**C**. For the subsequent substitution reaction, Cl in $^2$**C** must move to the reaction site, that is, C4, resulting in intermediate $^2$**D**, which is 4.7 kcal $mol^{-1}$ higher in energy than $^2$**C**. Orbital and spin analyses indicate that the *p* orbitals of Cl and carbon atoms (C4′ in $^2$**C** and C4 in $^2$**D**) overlap for electron delocalization, which stabilizes the radical (Supplementary Fig. 27). The higher energy of $^2$**D** compared to $^2$**C** can be attributed to the distortion of nitrobiphenyl, as the nitro group significantly deviates from the molecular plane by 10.1°. Although less stable, this deviation weakens the conjugation between the nitro group and benzene ring, thus activating nitrobiphenyl and facilitating the substitution reaction. The subsequent substitution of the nitro group with Cl occurs through a concerted transition state ($^2$**TS1**) with an activation barrier of 13.0 kcal $mol^{-1}$, affording $NO_2$ and the chlorobiphenyl product. In the absence of iron, chlorine radicals can be generated through the photolysis of chlorine gas, followed by a similar radical substitution reaction (Supplementary Fig. 27). The alternative reaction of triplet biradical nitrobiphenyl substrate and a chloride ion was also evaluated by DFT calculations (Supplementary Fig. 28). Its barrier is 14.3 kcal $mol^{-1}$ higher than that for the reaction with the chlorine radical, supporting the necessity of chlorine radicals for the efficient denitrative chlorination reaction.

## Conclusion

In summary, we developed a practical strategy for a general direct aromatic denitrative chlorination reaction, to substitute the $NO_2$ moiety under visible-light irradiation without any noble metals and additional photoredox catalysts, demonstrating a wide substrate scope and broad functional group tolerance. A wide range of electron-rich nitroarenes, unactivated nitro-heterocycles and nitroalkenes are well tolerated under this protocol. What is more, the reaction features operational simplicity and scalability, as a practical supplement for the construction of $C_{Ar}$–Cl bonds. Overall, the direct use of the $NO_2$ moiety as a leaving group under light irradiation to cleave the $C_{Ar}$–$NO_2$ bond offers a unique

approach for the arene modification of electron-unbiased nitroarenes, providing an alternative pathway for the transformation of nitroarenes.

## Online content

Any methods, additional references, Nature Portfolio reporting summaries, source data, extended data, supplementary information, acknowledgements, peer review information; details of author contributions and competing interests; and statements of data and code availability are available at https://doi.org/10.1038/s41557-024-01728-1.

## References


1. Ju, K. S. & Parales, R. E. Nitroaromatic compounds, from synthesis to biodegradation. *Microbiol. Mol. Biol. Rev.* **74**, 250–272 (2010).
2. Booth, G. *Nitro Compounds, Aromatic* (Wiley-VCH Verlag, 2000).
3. Sharma, K. *Nitro Compounds: Classification, Preparation, Properties, Reactions, Uses* (Wiley, 2023).
4. Amini, B. & Lowenkron, S. Aniline and its derivatives. *Kirk-Othmer Encyclopedia of Chemical Technology* Vol. 2, 783–809 (Wiley, 2003).
5. Olah, G. A., Malhotra, R. & Narang, S. C. Nitration: *Methods and Mechanism* 975–979 (World Scientific, 2003).
6. Nykaza, T. V. et al. Intermolecular reductive C–N cross coupling of nitroarenes and boronic acids by $P^{III}/P^{V}$=O catalysis. *J. Am. Chem. Soc.* **140**, 15200–15205 (2018).
7. Nykaza, T. V., Ramirez, A., Harrison, T. S., Luzung, M. R. & Radosevich, A.T. Biphilic organophosphorus-catalyzed intramolecular $C_{sp^2}$–H amination: evidence for a nitrenoid in catalytic cadogan cyclizations. *J. Am.Chem. Soc.* **140**, 3103–3113 (2018).
8. Nykaza, T. V., Li, G., Yang, J., Luzung, M. R. & Radosevich, A. T. $P^{III}/P^{V}$=O catalyzed cascade synthesis of N-functionalized azaheterocycles. *Angew. Chem. Int. Ed.* **59**, 4505–4510 (2020).
9. Li, G., Lavagnino, M. N., Ali, S. Z., Hu, S. & Radosevich, A. T. Tandem C/N-difunctionalization of nitroarenes: reductive amination and annulation by a ring expansion/contraction sequence. *J. Am. Chem. Soc.* **145**, 41–46 (2023).
10. Ryabchuk, P. et al. Cascade synthesis of pyrroles from nitroarenes with benign reductants using a heterogeneous cobalt catalyst. *Angew. Chem. Int. Ed.* **59**, 18679–18685 (2020).
11. Gui, J. et al. Practical olefin hydroamination with nitroarenes. *Science* **348**, 886–891 (2015).
12. Schwob, T. & Kempe, R. A reusable Co catalyst for the selective hydrogenation of functionalized nitroarenes and the direct synthesis of imines and benzimidazoles from nitroarenes and aldehydes. *Angew. Chem. Int. Ed.* **55**, 15175–15179 (2016).
13. Gkizis, P. L., Triandafillidi, I. & Kokotos, C. G. Nitroarenes: the rediscovery of their photochemistry opens new avenues in organic synthesis. *Chem* **9**, 3401–3414 (2023).
14. Paolillo, J. M., Duke, A. D., Gogarnoiu, E. S., Wise, D. E. & Parasram, M. Anaerobic hydroxylation of $C(sp^3)$–H bonds enabled by the synergistic nature of photoexcited nitroarenes. *J. Am. Chem. Soc.* **145**, 2794–2799 (2023).
15. Ruffoni, A., Hampton, C., Simonetti, M. & Leonori, D. Photoexcited nitroarenes for the oxidative cleavage of alkenes. *Nature* **610**, 81–86 (2022).
16. Hampton, C., Simonetti, M. & Leonori, D. Olefin dihydroxylation using nitroarenes as photoresponsive oxidants. *Angew. Chem. Int. Ed.* **62**, e202214508 (2023).
17. Wise, D. E. et al. Photoinduced oxygen transfer using nitroarenes for the anaerobic cleavage of alkenes. *J. Am. Chem. Soc.* **144**, 15437–15442 (2022).
18. Sanchez-Bento, R., Roure, B., Llaveria, J., Ruffoni, A. & Leonori, D. A strategy for ortho-phenylenediamine synthesis via dearomative-rearomative coupling of nitrobenzenes and amines. *Chem* **9**, 3685–3695 (2023).
19. Li, B., Ruffoni, A. & Leonori, D. A photochemical strategy for ortho-aminophenol synthesis via dearomative–rearomative coupling between aryl azides and alcohols. *Angew. Chem. Int. Ed.* **62**, e202310540 (2023).
20. Matador, E. et al. A photochemical strategy for the conversion of nitroarenes into rigidified pyrrolidine analogues. *J. Am. Chem. Soc.* **145**, 27810–27820 (2023).
21. Mykura, R. et al. Synthesis of polysubstituted azepanes by dearomative ring expansion of nitroarenes. *Nat. Chem.* **16**, 771–779 (2024).
22. Muto, K., Okita, T. & Yamaguchi, J. Transition-metal-catalyzed denitrative coupling of nitroarenes. *ACS Catal.* **10**, 9856–9871 (2020).
23. Mo, F., Qiu, D., Zhang, Y. & Wang, J. Renaissance of Sandmeyer-type reactions: conversion of aromatic C–N bonds into C–X bonds (X = B, Sn, P, or $CF_3$). *Acc. Chem. Res.* **51**, 496–506 (2018).
24. Mateos, J. et al. Nitrate reduction enables safer aryldiazonium chemistry. *Science* **384**, 446–452 (2024).
25. Bunnett, J. F. & Zahler, R. E. Aromatic nucleophilic substitution reactions. *Chem. Rev.* **49**, 273–412 (1951).
26. Yadav, M. R. et al. The Suzuki–Miyaura coupling of nitroarenes. *J. Am. Chem. Soc.* **139**, 9423–9426 (2017).
27. Inoue, F., Kashihara, M., Yadav, M. R. & Nakao, Y. Buchwald–Hartwig amination of nitroarenes. *Angew. Chem. Int. Ed.* **56**, 13307–13309 (2017).
28. Kashihara, M. & Nakao, Y. Cross-coupling reactions of nitroarenes. *Acc. Chem. Res.* **54**, 2928–2935 (2021).
29. Fráter, G. & Havinga, E. Photosubstitution reactions of nitronaphtalenes leading to chloronaphtalene. *Tetrahedron Lett.* **10**, 4603–4604 (1969).
30. Vink, I. A. J., Verheijdt, P. L., Cornelisse, J. & Havinga, E. Photoreactions of aromatic compounds—XXVI: photoinduced reactions of biphenyl and biphenyl derivatives with cyanide ion. *Tetrahedron* **28**, 5081–5087 (1972).
31. Pistritto, V. A., Liu, S. & Nicewicz, D. A. Mechanistic investigation into amination of unactivated arene via cation radical accelerated nucleophilic aromatic substitution. *J. Am. Chem. Soc.* **144**, 15118–15131 (2022).
32. Pistritto, V. A., Schutzbach-Horton, M. E. & Nicewicz, D. A. Nucleophilic aromatic substitution of unactivated fluoroarenes enabled by organic photoredox catalysis. *J. Am. Chem. Soc.* **142**, 17187–17194 (2020).
33. Tay, N. E. S. et al. $^{19}F$- and $^{18}F$-arene deoxyfluorination via organic photoredox-catalysed polarity-reversed nucleophilic aromatic substitution. *Nat. Catal.* **3**, 734–742 (2020).
34. Romero, N. A., Margrey, K. A., Tay, N. E. & Nicewicz, D. A. Site-selective arene C–H amination via photoredox catalysis. *Science* **349**, 1326–1330 (2015).
35. Juliá, F. Ligand-to-metal charge transfer (LMCT) photochemistry at 3*d*-metal complexes: an emerging tool for sustainable organic synthesis. *ChemCatChem* **14**, e202200916 (2022).
36. Song, S. et al. DMSO-catalysed late-stage chlorination of (hetero) arenes. *Nat. Catal.* **3**, 107–115 (2020).
37. Camelio, A. M. et al. Computational and experimental studies of phthaloyl peroxide-mediated hydroxylation of arenes yield a more reactive derivative, 4,5-dichlorophthaloyl peroxide. *J. Org. Chem.* **80**, 8084–8095 (2015).
38. Mo, F. et al. Gold catalyzed halogenation of aromatics by *N*-halosuccinimides. *Angew. Chem. Int. Ed.* **49**, 2028–2032 (2010).
39. Fosu, S. C., Hambira, C. M., Chen, A. D., Fuchs, J. R. & Nagib, D. A. Site-selective C–H functionalization of (hetero)arenes via transient, non-symmetric iodanes. *Chem* **5**, 417–428 (2019).
40. Wang, W. et al. Catalytic electrophilic halogenation of arenes with electron-withdrawing substitutents. *J. Am. Chem. Soc.* **144**, 13415–13425 (2022).

41. da Petruci, J. F. S., Tütüncü, E., Cardos, A. A. & Mizaikoff, B. Real-time and simultaneous monitoring of NO, $NO_2$, and $N_2O$ using substrate–integrated hollow waveguides coupled to a compact fourier transform infrared (FT-IR) spectrometer. *Appl. Spectrosc.* **73**, 98–103 (2019).
42. Tu, J., Hu, A., Guo, L. & Xia, W. Iron-catalyzed C($sp^3$)–H borylation, thiolation, and sulfinylation enabled by photoinduced ligand-to-metal charge transfer. *J. Am. Chem. Soc.* **145**, 7600–7611 (2023).
43. Steube, J. et al. Janus-type emission from a cyclometalated iron(III) complex. *Nat. Chem.* **15**, 468–474 (2023).
44. Abderrazak, Y., Bhattacharyya, A. & Reiser, O. Visible-light-induced homolysis of earth-abundant metal-substrate complexes: a complementary activation strategy in photoredox catalysis. *Angew. Chem. Int. Ed.* **60**, 21100–21115 (2021).
45. Chinchole, A., Henriquez, M. A., Cortes-Arriagada, D., Cabrera, A. R. & Reiser, O. Iron(III)-light-induced homolysis: a dual photocatalytic approach for the hydroacylation of alkenes using acyl radicals via direct HAT from aldehydes. *ACS Catal.* **12**, 13549–13554 (2022).

## Methods

Under an argon atmosphere, a 4 ml borosilicate vial equipped with a magnetic stir bar was charged with $FeCl_3$ (11.4 mg, 0.070 mmol, 35 mol%), oxone (69.3 mg, 0.20 mmol, 50 mol%), NaCl (35 mg, 0.60 mmol, 3.0 equiv.) and nitroarenes (0.20 mmol, 1.0 equiv.), and then 2.5 ml MeCN was added. The reaction mixture that was irradiated with the 390 nm LEDs was stirred at 75 °C for 48 h. Then the reaction mixture was transferred to a flask with ethyl acetate, and the volatiles was removed under vacuum. The residues were then purified by flash column chromatography on silica gel, eluting with hexanes to afford products.

## Data availability

The data supporting the findings of this study are available within the paper and its Supplementary Information. Crystallographic data for compound **52** have been deposited at the Cambridge Crystallographic Data Centre (CCDC) under deposition number 2341039. These data can be obtained free of charge from the CCDC (http://www.ccdc.cam.ac.uk/data_request/cif).

## Acknowledgements

We thank J. Wang (PKU) for the high-resolution MS testing and Z. Luo (Central China Normal University (CCNU)) for the IR testing. We thank X. Meng (CCNU) for X-ray structure refinement. We thank L. Chen (CCNU) for electron paramagnetic resonance measurement. We also thank Y. Xu (Peking University) and G. Wu (Huazhong University of Science and Technology) for helpful discussion about the project. We are grateful to the Knowledge Innovation Program of the Wuhan-Shuguang Project (2023020201020308; F.Y.); the Cultivation Program of Wuhan Institute of Photochemistry and Technology (GHY2023KF003; F.Y.); the National Natural Science Foundation of China (22173077 and 22422110; G.-J.C.) and the Guangdong Basic and Applied Basic Research Foundation (2023B1515020052; G.-J.C.) for financial support; and CCNU for startup funding (F.Y.).

## Author contributions

T.L. developed the reaction methods and investigated the mechanism. T.L., Y.W. and W.Z. explored the substrate scope. Z.L. performed the DFT calculation. R.S, G.-J.C. and F.Y. prepared the paper. F.Y. directed the project.

## Competing interests

The authors declare no competing interests.

## Additional information

**Supplementary information** The online version contains supplementary material available at https://doi.org/10.1038/s41557-024-01728-1.

**Correspondence and requests for materials** should be addressed to Gui-Juan Cheng or Fei Ye.

**Peer review information** *Nature Chemistry* thanks Wei Guan and the other, anonymous, reviewer(s) for their contribution to the peer review of this work.